Korean J. Chem. Eng., 32(9), 1789-1797 (2015)
DOI: 10.1007/s11814-014-0376-9

pISSN: 0256-1115
eISSN: 1975-7220

Hydrothermal carbonization of oil palm shell

Sabzoi Nizamuddin*, Natesan Subramanian Jayakumar*,†, Jaya Narayan Sahu, Poobalan Ganesan***, Abdul Waheed Bhutto****, and Nabisab Mujawar Mubarak*,*****

*Department of Chemical Engineering, Faculty of Engineering, University of Malaya, Kuala Lumpur 50603, Malaysia
**Department of Petroleum and Chemical Engineering, Faculty of Engineering, Institut Teknologi Brunei, Tungku Gadong, P. O. Box 2909, Brunei Darussalam
***Department of Mechanical Engineering, Faculty of Engineering, University of Malaya, Kuala Lumpur 50603, Malaysia
****Department of Chemical Engineering, Dawood University of Engineering and Technology, M.A Jinnah Road, Karachi, Pakistan
*****Department of Chemical and Petroleum Engineering, Faculty of Engineering, UCSI University, Kuala Lumpur 56000, Malaysia
(*Received 29 July 2014 • accepted 17 December 2014*)

Abstract−Palm shell is one of the most plentiful wastes of the palm oil mill industry. This study identifies the capability of hydrothermal carbonization process (HTC) to convert palm shell into high energy hydrochar. The influence of reaction time and reaction temperature of the HTC process was investigated. The process parameters selected were temperature 200 °C to 240 °C, time 10 to 60 min, and water to biomass ratio was fixed at 10 : 1 by weight %. Fourier transform infrared (FTIR), elemental, proximate, Burner Emmett and Teller (BET), thermo-gravimetric (TGA) analyses were performed to characterize the product and the feed. The heating value (HHV) was increased from 12.24 MJ/kg (raw palm shell) to 22.11 MJ/kg (hydrochar produced at 240 °C and 60 min). The hydrochar yield exhibited a higher degree inverse proportionality with temperature and reaction time. Elemental analysis revealed an increase in carbon percentage and a proportional decrease in hydrogen and oxygen contents which caused higher value of HHV. The dehydration and decarboxylation reactions take place at higher temperatures during HTC resulting in the increase of carbon and decrease in oxygen values of hydrochar. The FESEM results reveal that the structure of raw palm shell was decomposed by HTC process. The pores on the surface of hydrochar increased as compared to the raw palm shell.

Keywords: Hydrothermal Carbonization, Palm Shell, Hydrochar, Characterization, Renewable Energy

INTRODUCTION

Emission of several greenhouse gases (GHGs), especially carbon dioxide (CO_2), from petroleum products is severely deteriorating the environment. Scientifically provided data show that further deterioration of the environment may result in a threat of extinction of millions of creatures [1]. Moreover, dearth in availability and unstable prices are a few other drawbacks of petroleum fuels. Petroleum products need to be substituted by renewable energy resources. It has been observed that among the available renewable energy resources that can be a substitute for fossil fuels, biomass is second to none. Abundance, environmentally friendly behavior, sustainability and low cost have promoted biomass to gain more attention and recognition. Certain other benefits of biomass include CO_2 neutral substitute of fossil fuels because the burning of biomass as a fuel is the reversal of photosynthesis process [2,3]. It is expected that with upgraded technology in future, biomass will give out only 15 to 18 g/kWh of CO_2. In addition to that SOx and NOx trimmer, biodiversity and public forecasts are also considerable merits of the biomass. Utilization of biomass waste will also decrease dumping cost, for instance incineration of solid municipal waste lessening up to 90% waste by volume and generating fuels or biomass based chemicals.

A number of products can be obtained from biomass, either completely or partially such as fuels (solid, liquid, gases), pharmaceuticals, resins, solvents, polymer, paints, inks and cosmetics [4,5]. To achieve these products, biomass can be abundantly extracted from various resources, out of which agricultural waste is a key resource. Agricultural wastes are mainly focused due to abundance, environmentally supporting behavior and low cost [6,7]. Recently, oil palm has been recognized as the top available form of agricultural product in wet and humid areas like Malaysia [8,9]. It has various applications in industries such as soap manufacturing and cooking oil industries. Oil palm produces large amounts of wastes like fiber, empty fruit bunch (EFB), fronds, trunks and shell. Only in Malaysia, there are about 362 oil palm mills which process about 82 million tons of fresh fruit bunches and produce about 33 million tons of waste every year [10,11]. Significant waste from palm oil is palm shell. Major components of palm shell include celluloses, hemicelluloses and lignin with elemental composition of 49.75 wt% carbon, 44.86 wt% oxygen, 5.32 wt% hydrogen, 0.08 wt% nitrogen and 0.16 wt% of sulfur [12]. These wastes cause many problems such as bad odor, dumping problems and hazardous methane gas from the decomposition process [13]. Various studies have been under-

†To whom correspondence should be addressed.
E-mail: jaya_kumar@um.edu.my

taken to find solutions to these problems like direct burning, energy recovery and activated carbon production [14,15]. One approach is to convert palm shell into hydrochar using hydrothermal carbonization (HTC). Application of HTC to waste streams will help to minimize the waste together with mitigation of greenhouse gas emissions [16]. Note that palm shell possesses low energy which can be enhanced by applying HTC process to convert it into high energy hydrochar. HTC process is a promising route for the production of higher density fuels and carbonaceous functional materials. Additionally, the lignocellulosic composition (lignin - 49%, cellulose - 31% and hemicellulose - 20% [17]) of the oil palm shell makes it a suitable candidate for solid fuel production. Hydrochar applications include CO_2 sequestrations, energy source generation, super capacitors, anode and cathode materials for fuel cells and batteries and soil conditioning [18-20]. The HTC process may be classified as direct HTC and catalytic HTC process. In the direct HTC process, only water and feed are heated in a reactor at different temperatures in the absence of the catalyst, whereas in the catalytic HTC process the catalyst is added. In this study, the direct HTC process was applied to palm shell in an autoclave batch reactor at 200 to 240 °C for 10 to 60 minutes. The main objective of this study is to investigate the ability of the direct HTC process for the production of hydrochar from palm shell at moderate temperature and time range and to characterize hydrochars as to find the effect of HTC on oil palm shell. The produced hydrochar was characterized using elemental composition, heating value, proximate, Fourier transform infrared (FTIR), Burner Emmett and Teller (BET), thermo-gravimetric (TGA) and Field emission scanning electron microscopy (FESEM) analyses to evaluate the feasibility of hydrochar for solid fuel applications.

MATERIALS AND METHODS

1. Raw Materials

The raw palm shell was supplied by the Seri Ulu Langat Palm Oil Mill Dengkil, Selangor, Malaysia. It was washed several times with tap water and finally with the distilled water to remove dirt and other impurities. Later, the palm shell sample was dried at 105 °C for 24 hours to remove moisture present on the surface. The dried palm shell was ground and sieved to the size as shown in Table 1.

2. Production of Hydrochar Using HTC Process

HTC process was carried out in an autoclave batch reactor. The reactor was loaded with 500 g of feed consisting of dried raw palm shell and distilled water with a biomass to water ratio of 1 : 10 wt%. Excess water was provided for complete immersion of feed during the reaction. The reactor was purged with nitrogen at three bars for 5 minutes for confirming that the reactor was closed tightly and there was no leakage. After that, the purging of nitrogen was done at 10 bars to avoid the water vaporization during heating. The stirrer speed was set to 400 rotations per minute (rpm). Experiments were carried out at 200 to 240 °C and reaction time was set between 10 to 60 min. Temperature, pressure and stirrer speed were controlled by the online system. After the completion of the reaction, the reactor was cooled to room temperature. The gaseous product, being negligible, was vented. The slurry containing solid and liquid products was filtered and separated. The solid product was dried at the 105 °C for 24 hours and further characterized.

Table 1. Size distribution of raw palm shell used for hydrochar production

Particle size (μm)	Weight distribution %
x<500	6.1
500<x<1000	5.5
1000<x<1400	4.8
1400<x<2000	8.9
2000<x<2500	5.9
x<2500	68.8

3. Experimental Setup

The whole experimental work was carried out in a high pressure stainless steel autoclave reactor with a capacity of 1 L as shown in Fig. 1. The reactor was designed to achieve maximum temperature and pressure conditions as 500 °C and 100 bars, respectively. The reactor was fitted with a safety rupture disc. These sorts of discs burst in case of exceeding temperature and pressure values. Automatic proportional integral derivative (PID) controlled 2250 Watt ceramic heater was used to heat up the reactor. A turbine stirrer was used to mix the reactants uniformly during the reaction. Stainless steel thermocouple and a pressure gauge were used for the measurement of temperature and pressure respectively. Continuous water was circulated to cool down the instruments and joints of the reactor in combination with another cooling coil to reduce the temperature of the reactor abruptly after completion of the reaction.

4. Characterization of Raw Palm Shell and Hydrochar

The chemical and physical characteristics of the raw palm shell and hydrochar were investigated to examine the effect of HTC process parameters on the raw palm shell. Elemental analysis was examined in PerkinElmer Series II CHNS/O Analyzer (Model: 2400) to measure the carbon, hydrogen, nitrogen and oxygen values. The FTIR analysis was performed to determine the atomic bonding on surface of hydrochar by Fourier transform infrared spectroscopy (Bruker, IFS66v/S). The surface morphology of raw palm shell and hydrochar produced at different temperatures and 60 min reaction time was determined by FESEM, (Brand: Zeiss, Model: Auriga). The surface area was determined by Burner Emmett and Teller (BET) (Brand: Quanta Chrome, Model: Autos orb 6B). Thermo gravimetric analysis (TGA) was carried out in TGA-Q500.

5. Yield % of Hydrochar

The yield of hydrochar at different reaction temperature and run time is shown in Fig. 2. The yield percentage was calculated by the equation

$$\text{Hydrochar Yield\%} = [W_P/W_f] \times 100 \quad (1)$$

where, W_p is the weight of dry hydrochar product and W_f is weight of dry palm shell feed.

RESULTS AND DISCUSSION

1. Effect of Reaction Temperature and Time on Yield %

The yield % of hydrochar and bio-oil is shown in Fig. 2. The yield of hydrochar was decreased at higher temperatures and reaction time due to thermal degradation of palm shell. The higher yield

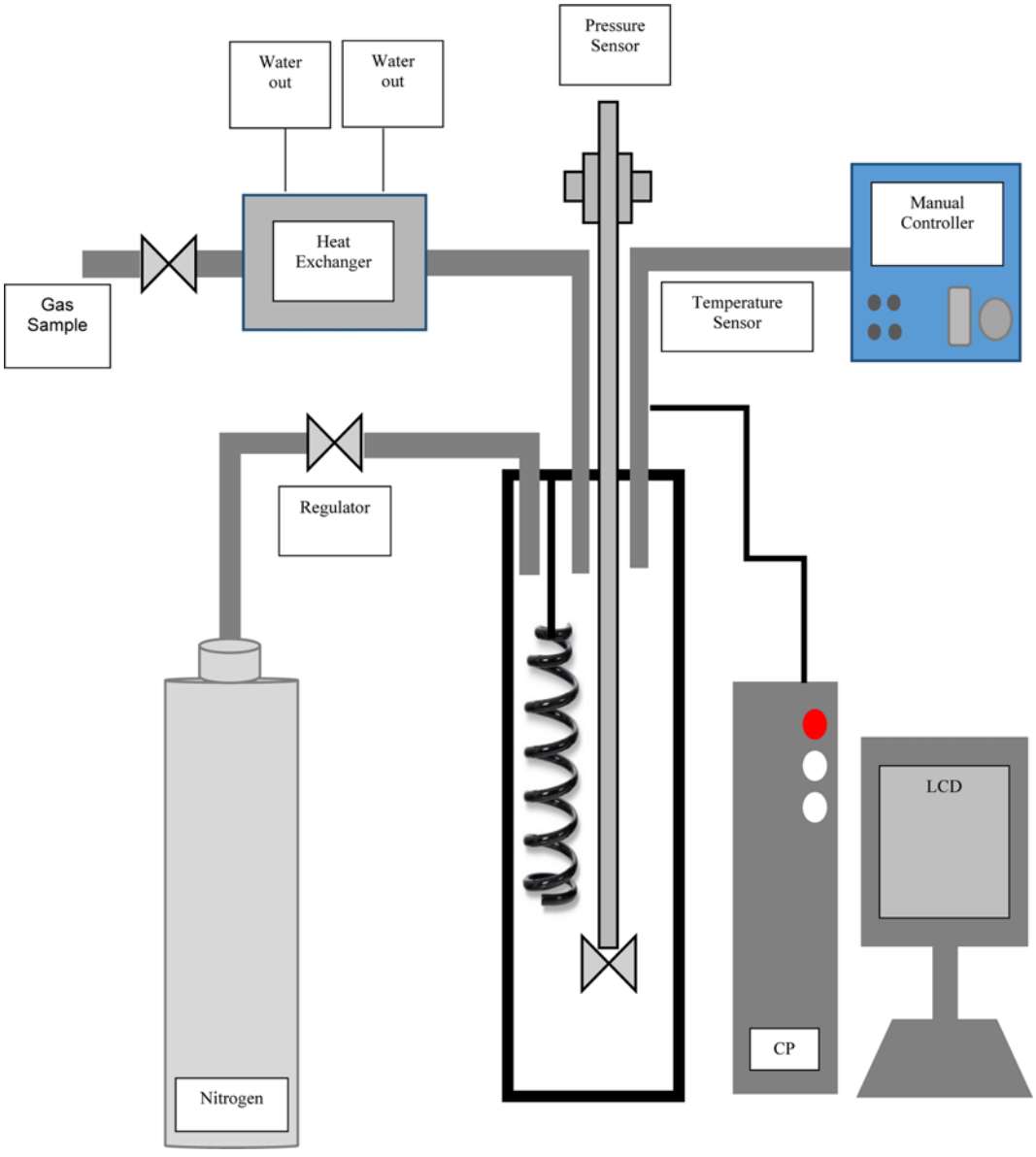

Fig. 1. Schematic of high pressure batch reactor used for production of hydrochar from HTC process.

percentage was obtained at lower temperatures and lower reaction times, whereas lower yield was obtained at higher temperatures and reaction times. About 60% mass was recovered at the 200 °C for 10 minutes and this amount went down up to 43% at 240 °C and 60 min. A sudden decline in solid yield was perceived with an increase in temperature, which may be due to any of three reasons: (i) higher primary decomposition of feed at higher temperature, (ii) by secondary decomposition of solid residue, and (iii) due to high solubilization of components in hydrolysis liquors [21,22]. These results are justified by previous research work [23-25].

Unlike solid product, yield % of bio-oil increased gradually with an increase in reaction time and temperature. 12.16% of bio-oil was observed at 200 °C and 10 min reaction time, whereas 35.36% of bio-oil was produced at 240 °C and 60 min reaction time. As the temperature increased, the yields of both liquid and gaseous products increased due to an increase in decomposition rate of palm shell [26]. The previous studies reported that more oil and gases are produced with increasing temperature up to a point [27]. The previous studies related to reaction time also observed a similar trend with our study. The liquid yield increased, whereas the solid yield decreased with increasing reaction time from 10 min to 60 min at 360 °C [28].

2. HHV, Ultimate and Proximate Analyses

HHV values, proximate and ultimate analyses of hydrochar product at different reaction conditions are listed and compared to those of coal in Table 2. The HTC significantly influenced raw palm shell. HHVs of raw palm shell and hydrochars were measured with a bomb calorimeter (IKA C2000 basic). The HHV values of hydrochar product were increased as compared to raw palm shell because of increasing carbon content at higher temperatures. The increased carbon content at higher temperature improved the heating value of the product from 12.24 MJ/kg (palm shell feed) to 22.11 MJ/kg

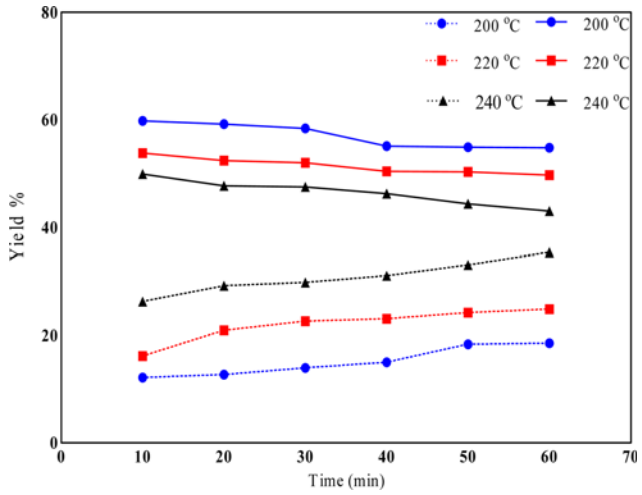

Fig. 2. Yield % of solid (—) and liquid (…) products obtained at 200 °C, 220 °C, and 240 °C for 10 to 60 min reaction time.

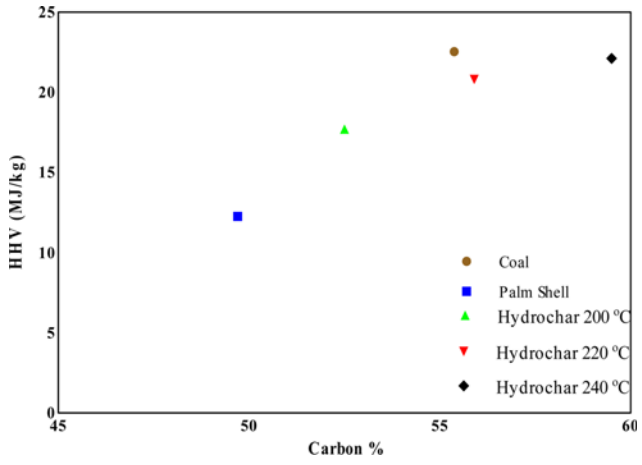

Fig. 3. Relationship between carbon content and calorific value of raw feed and hydrochar.

(hydrochar) at 240 °C and 60 min run time, which is approximately equivalent to the heating value of coal. These results confirm that the solid product obtained through the HTC process has suitable properties to be used as a solid fuel.

The correlation between the calorific value and the carbon content of the raw palm shell and hydrochar obtained at different temperature ranges for 60 min reaction time as shown in Fig. 3. It can

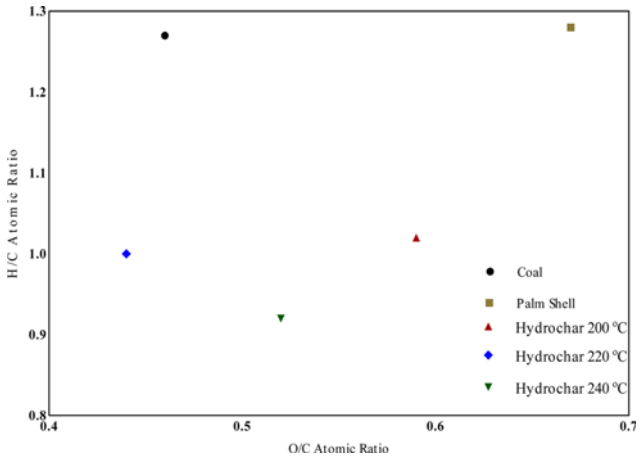

Fig. 4. Van Krevelen diagram of coal, raw palm shell and hydrochars produced at 200 °C, 220 °C, 240 °C and 60 min.

be concluded that the carbon value is proportional to heating value. The statement that the carbon increment in the product will be at the detriment of hydrogen content, which increases the combustion ability of product [29], is proven by the data given in Fig. 3.

The ultimate analysis aims to determine the composition and quantity of the gas emitted during the combustion as well as the amount of oxygen required for the burning of the biomass or fuels [30]. The carbon content of hydrochar was improved by increasing the temperature, while hydrogen and oxygen content were decreased with the rise in temperature. The carbon content (52.5, 55.9 and 59.5%) of solid hydrochar at different temperatures was found greater than that of raw palm shell (49.7%). On the other hand, the hydrogen (4.5, 4.3 and 5%) and oxygen contents (41.8, 38.8 and 34.8%) of hydrochar were decreased as compared to those of (5.3% and 44.8% respectively) of palm shell. These phenomena of ultimate analysis are attributed to increase in temperature and deoxygenating reactions (decarboxylation and dehydration reactions) occurring during the HTC process [31]. Both decarboxylation and dehydration reactions take place during the HTC process [32,33]. Decrease in hydrogen and oxygen content with an increase in temperature corresponds to the scission of weak bonds within char structure favored by the higher reaction temperature [34]. Carbon content in hydrochars depends on the carbon content of feed as well [35]. A similar trend for ultimate analysis of hydrochar was discussed and observed by Y. Basiron et al. [9].

Oxygen to carbon (O/C) and hydrogen to carbon (H/C) atomic

Table 2. Elemental, proximate analyses and HHV values of coal [39], raw palm shell [43] and produced hydrochar of palm shell at 200 °C, 220 °C, 240 °C and 60 minutes reaction time

Material	Temp. (°C)	Proximate analysis %				Ultimate analysis %					HHV (MJ/Kg)
		FC	VM	Moisture	Ash	C	H	N	S	O (diff)	
Coal	0	40.7	34.8	15.1	9.3	55.4	5.9	2.5	2.2	34.1	22.5
Palm shell	0	13.8	74.3	4.7	7.2	49.7	5.3	0.8	0.2	44.8	12.2
Hydrochar	200	31.4	53.5	5.1	10.0	52.5	4.5	1.0	0.2	41.8	17.7
Hydrochar	220	39.1	52.6	4.9	3.4	55.9	4.3	0.9	0.2	38.8	20.8
Hydrochar	240	40.6	45.9	4.1	9.3	59.5	5.0	0.5	0.2	34.8	22.1

ratios of coal, raw palm shell and hydrochar are presented in Fig. 4, van Krevelen diagram, to validate the production of carbon rich materials from carbohydrate materials [36]. Generally, lower H/C and O/C ratios are desired for a good fuel because of reduced energy loss, water vapor and smoke during combustion process [37]. It is evident from the Fig. 4 that both O/C and H/C ratios of solid hydrochar were decreased with the increase in temperature. The higher temperature promotes dehydration and decarboxylation reactions, which results in a decreased O/C ratio. The decrease in H/C and O/C atomic ratios may be because of exothermic oxidation of hydrogen and carbon to H_2O, CO and CO_2 at higher temperatures [38]. Similar results of HTC were observed for EFB, cellulose, sucrose, starch, glucose and agricultural biomass by a number of researchers [33,39-41].

Proximate analysis is supposed to find the ratio of combustible substances (fixed carbon and volatile matter) to noncombustible constituents (ash and moisture content), which enables one to determine the energy content of biomass or fuels. The higher amount of volatile matter in biomass influences its direct combustion and co-combustion with coal resulting in decreased performance of combustion and enhanced emissions of pollutants [42]. Proximate analysis results show that there was a significant decrease in volatile matter, from 74.30% to 45.95% and an increase in fixed carbon content from 13.80% to 40.6%. The increase in fixed carbon value is credited to the release of volatile matter occurred during HTC [43]. It is expected that biomass degrades significantly at higher temperatures resulting removal of volatile matters in more quantity [44]. Fixed carbon represents the amount of carbon which is not easily biodegraded and has a potential for ground burial for carbon credits [35]. The higher value of HHV of hydrochar in this study is attributed to amount of fixed carbon and volatile matter.

3. FTIR Analysis of Feed and Hydrochar

FTIR analysis through FTIR spectra on the wave number ranges from 4,000 to 400 cm^{-1} was carried out to analyze the surface functional groups of palm shell and hydrochar produced by HTC process at different reaction conditions. Such spectra of compounds provide information regarding the existing bonds and also show the molecular structure of that specific compound [45]. The spectral data for the raw palm shell and solid product obtained by the FTIR analysis is given in Fig. 5. The absorbance peaks observed for hydrochar were almost similar to that for a raw palm shell. The

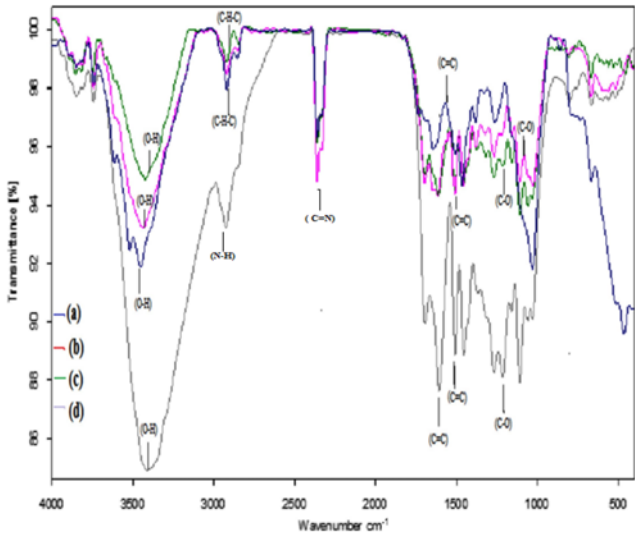

Fig. 5. Superimposed FTIR analysis of (a) raw palm shell and hydrochar (b) at 200 °C, (c) at 220 °C and (d) at 240 °C for 60 min.

peak of -OH groups was recognized approximately at 3,412-3,452 cm^{-1}. It is due to overlaying of the N-H bond of amino groups [46] and decrease in O-H bond due to high temperatures, which indicates that the raw material was dehydrated and the water present in solids was removed. A few similar peaks were noted at 2,923 cm^{-1}, and 2,919 cm^{-1}, 2,920 cm^{-1}, 2,924 cm^{-1} due to C-H stretching vibrations of $CH/CH_2/CH_3$ [46]. These peaks were found to be lower in solid product as compared to the raw palm shell. It indicates that hydrogen has been removed considerably by HTC process. The bond observed at 2,360 cm^{-1} represents alkynes. The peak around 1,110 cm^{-1} and 1,030 cm^{-1} is because of Si-O-Si stretching vibrations. A summary of the FTIR spectra analysis is given in Table 3.

4. FESEM Analysis of Feed and Hydrochar

FESEM is a potential technique used to study the morphological structure of biomass and samples produced from biomass through different treatments. The morphological structures of raw palm shell and solid product were assessed through FESEM to determine the particle surface structure and compared in Fig. 6. The palm shell has a rough surface with fewer pores. At high tempera-

Table 3. Wave number and ascription of the principle bands in FTIR spectra of hydrochar and raw palm shell

Wave number (cm^{-1})	Assignment	Palm shell	Hydrochar at 200 °C	Hydrochar at 220 °C	Hydrochar at 240 °C
3500-3300	Alcohols & Phenols, O-H Stretching	3452.26	3440.25	3422.75	3412.74
3000-2850	Alkanes, H-C-H Asymmetric & symmetric	2919.14	2919.56	2920.61	2924.68
1650-1550	Aromatic C=C stretching	1645.91	1615.94	1612.78	1607
1550-1260	Carboxylic acids & derivatives, C-O bending	1467.03	1510.98	1510.88	1509.68
			1458.20	1457.26	1456.04
			1381.76	1269.57	1214.71
			1270.07		
850-500	Aromatic substitution by aliphatic groups	-	667.59	668.83	667.28
					80

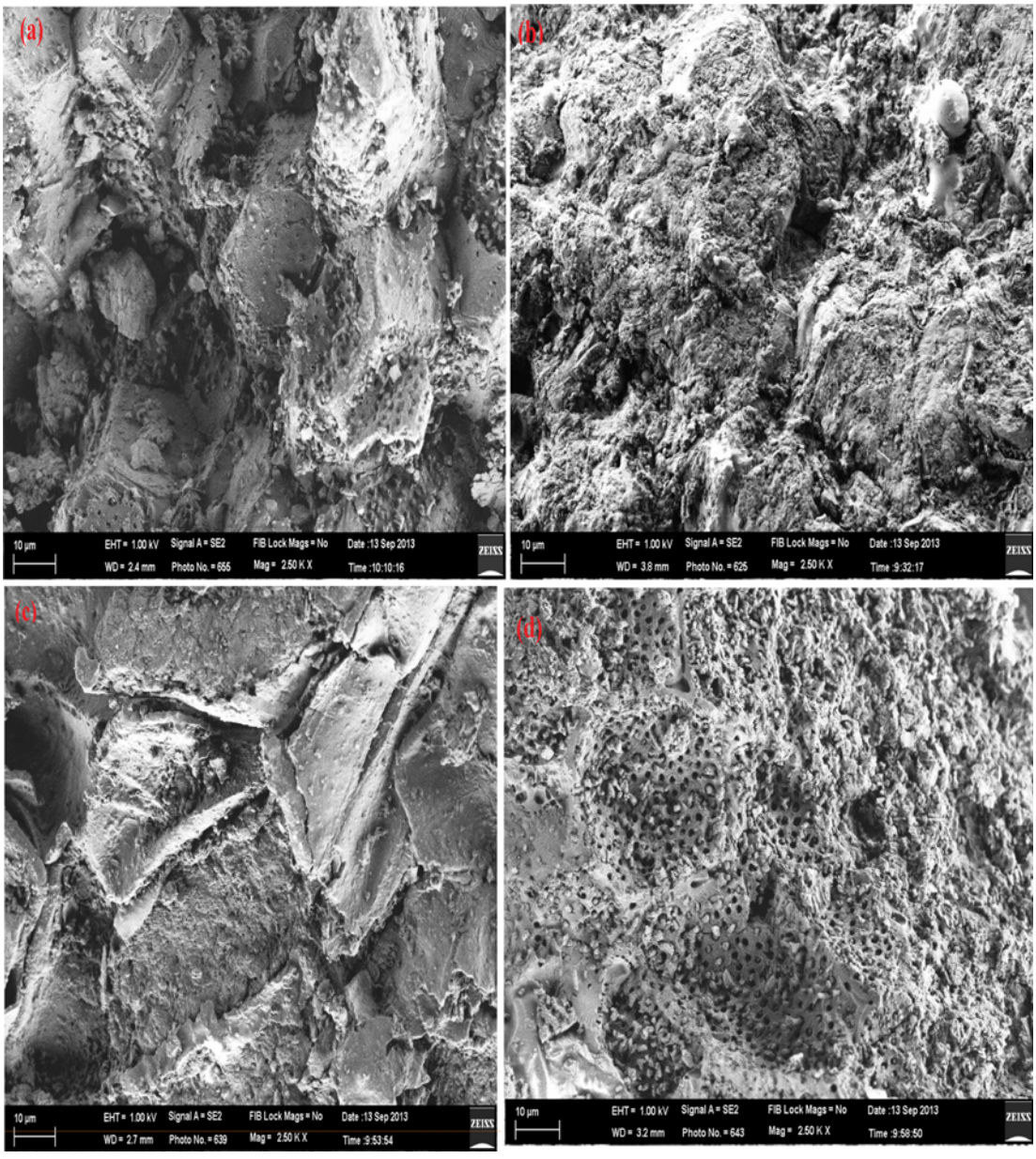

Fig. 6. FESEM images of (a) raw palm shell and hydrochars at (b) 200 °C, (c) 220 °C and (d) 240 °C for 60 min.

ture, the pores on the surface of hydrochar product were highly increased and resulted in more compact surface with large surface area. It proves that temperature is the most effective parameter, because more pores were generated on the surface of hydrochar produced at the 240 °C as compared to hydrochar produced at lower temperatures. The small particles adhered to the surface of palm shell, and after conducting the HTC process, some particles were removed from the surface and it was confirmed that the structure of raw palm shell was eroded. With increase in temperature, decomposition of biomass increases and the basic layers of biomass are more exposed with temperature improving the porosity of char. The higher temperatures destroy the walls between adjacent pores, resulting in the enlargement of pores [47]. Chars produced at higher temperatures contained several holes and cracks due to the evolution of volatiles with temperature increase [44]. The samples of chars produced at higher temperatures have higher micropore volume [48]. Similar results are observed from FESEM analysis of hydrochar of EFB [13]. The structure of biomass is altered significantly with heating rate [49]. The FESEM results confirm the validity of the BET results discussed in Table 4.

Table 4. BET Characteristics of raw pal shell [60] and hydrochar

Material	Av. pore diameter (Å)	BET surface area (m^2/g)	Total pore volume (cm^3/g)
Raw palm shell	45.1133	0.3106	0.001292
Hydrochar (200 °C)	131.5385	4.4747	0.014715
Hydrochar (220 °C)	200.8129	5.2483	0.026348
Hydrochar (240 °C)	239.803	10.9022	0.039202

5. BET Analysis of Feed and Hydrochar

Physical characterization of produced hydrochar was analyzed using BET (Brand: Quanta Chrome, Model: Autos orb 6B). Total pore volume of prepared sample was determined by the adsorbed amount of relative pressure (P/P_o) of 0.995, while pore size distribution in mesoporous range was calculated from the desorption branches of isotherms using the Barrett-Joyner-Halenda (BJH) model [16]. The surface area of the raw palm shell and produced hydrochar at different conditions is shown in Table 4. The results of BET analysis reveal that the BET surface area, total pore volume and average pore diameter of hydrochar product are improved and increased than those of the raw palm shell. The increase in BET characteristics can be due to the reaction temperature and time, which disintegrated the fibrous structure of raw palm shell and produced the number of pores in hydrochar. The rupture of the fibers and pore size on the surface of EFB were observed to increase in surface area with increase in temperature [13]. The increase in surface area of hydrochars with increase in temperature is because of the release of volatiles from biomass at higher temperatures [44]. The effect of temperature was studied in the BET surface area of pistachio nut shells, and it was observed that the BET surface area was improved by increasing the temperature because of increased volatiles evolution, which ultimately increased the pore development of hydrochar [50]. An increase in temperature causes widening of pore structure of biomass resulting in an increase in a BET surface area of hydrochars [51]. At higher temperatures of carbonization, total the pore volume and BET surface area of chars were increased, indicating that the chars produced at higher temperatures have more developed pore structure [52]. The accuracy of the results of this study is confirmed by previously reported studies [36,39]. Furthermore, the improvement in the surface area and porosity of hydrochar was required to make it more suitable for further applications, such as super capacitors for electrical energy storage or hydrogen storage. A combination of thermal and chemical activation is one of the ways to increase surface area [53].

6. TGA Analysis of Hydrochar

Thermal gravimetric analysis (TGA) is an efficient method to study the thermal and combustion performance of different materials, including biomass, coal and their blends by determining the weight change of material under the set value of temperature in a controlled atmosphere [39,54,55]. TGA for raw palm shell and hydrochars produced at 200 °C, 220 °C and 240 °C for 60 minutes reaction time was carried out in TGA-Q500 to measure and compare the thermal behavior and weight loss kinetics of hydrochar with flow of pure nitrogen (99.999%). 10 mg of sample was placed in a pan. The decomposition behavior of lignocellulosic biomass may be divided into four sections: (i) Removal of water content and light volatile components which occur at a temperature lower than 120 °C, (ii) degradation of hemicellulose takes place at the 220-315 °C, (iii) decomposition of cellulose and lignin at 315-400 °C, and (iv) degradation of lignin at >450 °C [56,57]. Fig. 7 shows the variation in weight loss with respect to temperature. Weight loss kinetics was almost similar for palm shell and hydrochars. Minor weight loss was observed between 50-100 °C, which corresponds to the removal

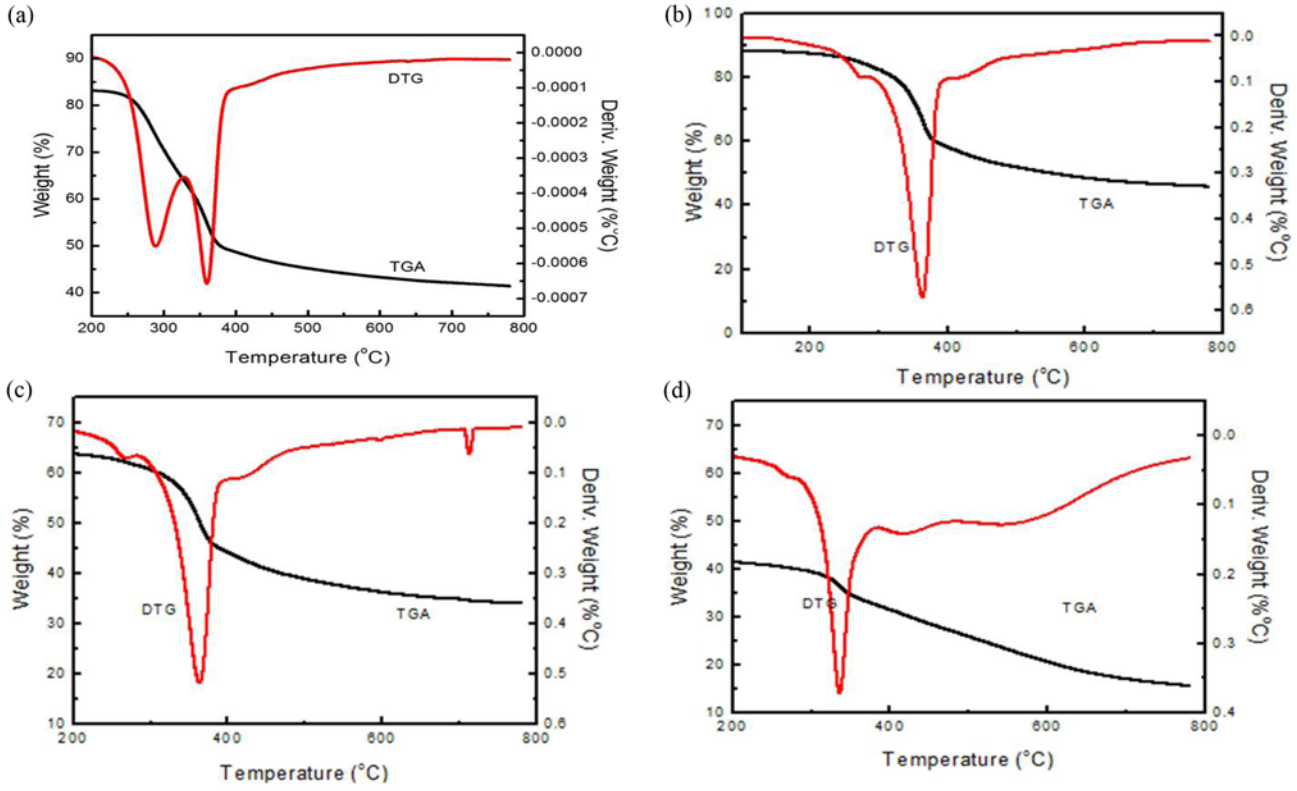

Fig. 7. Thermo gravimetric analysis (TGA) with DTG curves of (a) raw palm shell, (b) hydrochar at 200 °C, (c) hydrochar at 220 °C and (d) hydrochar at 240 °C.

of water absorbed; and from 200-750 °C, a fast rate of decomposition was observed, which is attributed to decomposition and pyrolysis of hemicellulose and cellulose. Also, the lower lignin content is inferred from the less marked decomposition at higher temperatures [55,58]. The weight loss taking place at 190-305 °C is because of pyrolysis of hemicellulose, whereas the pyrolysis of lignin and cellulose occurs at 305 °C-404 °C [52]. The profile between 750-850 °C remained almost flat, indicating the removal of all volatiles, hence remained as a residue.

The temperatures at which maximum rate of weight loss takes place are defined by the position of peaks in the DTG curve. The first DTG peak for raw palm shell is observed at ~290 °C, which is probably due to the decomposition of hemicellulose [59]. The second peak for the raw palm shell was observed at ~350 °C, which is attributed to the decomposition of cellulose [60]. The combustion of raw palm shell involves mainly combustion of volatile matter, which ignited at lower temperature due to its high reactivity. The rapid weight loss of palm shell at lower temperature range suggests that an incomplete combustion took place with low efficiency, causing high pollutant emissions [61]. DTG curve peaks for hydrochars were observed at 360-380 °C, suggesting that the thermal stability increased with increase in temperature. At the elevated combustion temperature range for hydrochars, minimized emission of pollutants is also expected by use of hydrochars.

CONCLUSIONS

The yield percentage of solid product was decreased with increasing temperature and run time because of the higher rate of liquefaction. Based upon obtained results, by HTC of raw palm shell, the production of hydrochar during the HTC reaction is influenced by both temperature as well as reaction time, hence the reaction time and the reaction temperature were found to be the key factors influencing the HTC process.

With the results of characterization of solid product, the rate of dehydration reaction and decarboxylation reaction was increased by increasing the temperature and reaction duration. The heating value improved up to 22.11 MJ/kg as compared to the heating value of feed palm shell 12.24 MJ/kg. The carbon content was increased in contrast to oxygen and hydrogen content, which were decreased because of the dehydration and decarboxylation reactions; hence the HTC process converted a low carbon feed into a product with high carbon content and high calorific value.

ACKNOWLEDGEMENT

This research is financially supported by University of Malaya, Ministry of Higher Education High Impact Research (UM.C/HIR/MOHE/ENG/20).

REFERENCES

1. S. H. Shuit, K. T. Tan, K. Lee and A. Kamaruddin, *Energy*, **34**, 1225 (2009).
2. A. Demirbaş, *Energy Convers. Manage.*, **42**, 1357 (2001).
3. J. Twidell, *Renew. Energy World*, **1**, 38 (1998).
4. A. Bridgwater and G. Peacocke, *Renew. Sustain. Energy Rev.*, **4**, 1 (2000).
5. K. Maher and D. Bressler, *Bioresour. Technol.*, **98**, 2351 (2007).
6. C. N. Hamelinck, G. v. Hooijdonk and A. P. Faaij, *Biomass. Bioenergy*, **28**, 384 (2005).
7. C. E. Wyman, *Bioresour. Technol.*, **50**, 3 (1994).
8. N. Mubarak, A. Kundu, J. Sahu, E. Abdullah and N. Jayakumar, *Biomass. Bioenergy*, **61**, 265 (2014).
9. Y. Basiron, *Eur. J. Lipid. Sci. Technol.*, **109**, 289 (2007).
10. C. S. Goh, K. T. Tan, K. T. Lee and S. Bhatia, *Bioresour. Technol.*, **101**, 4834 (2010).
11. A. Rahman Mohamed and K. T. Lee, *Energy Policy*, **34**, 2388 (2006).
12. F. Abnisa, W. Daud, W. Husin and J. Sahu, *Biomass. Bioenergy*, **35**, 1863 (2011).
13. S. S. Jamari and J. R. Howse, *Biomass. Bioenergy*, **47**, 82 (2012).
14. K. Mae, I. Hasegawa, N. Sakai and K. Miura, *Energy Fuel*, **14**, 1212 (2000).
15. C. W. Kean, J. N. Sahu and W. W. Daud, *BioResources.*, **8**, 1831 (2013).
16. G. K. Parshetti, S. Kent Hoekman and R. Balasubramanian, *Bioresour. Technol.*, **135**, 683 (2013).
17. A. A. Salema and F. N. Ani, *J. Anal. Appl. Pyrol.*, **96**, 162 (2012).
18. K. Wiedner, C. Rumpel, C. Steiner, A. Pozzi, R. Maas and B. Glaser, *Biomass. Bioenergy*, **59**, 264 (2013).
19. X. Lu, P. J. Pellechia, J. R. Flora and N. D. Berge, *Bioresour. Technol.*, **138**, 180 (2013).
20. A. Kruse, A. Funke and M.-M. Titirici, *Curr. Opin. Chem. Biol.*, **17**, 515 (2013).
21. S. Xiu, A. Shahbazi, V. Shirley and D. Cheng, *J. Anal. Appl. Pyrol.*, **88**, 73 (2010).
22. L.-P. Xiao, Z.-J. Shi, F. Xu and R.-C. Sun, *Bioresour. Technol.*, **118**, 619 (2012).
23. X. Lu, P. J. Pellechia, J. R. Flora and N. D. Berge, *Bioresour. Technol.*, **138**, 180 (2013).
24. Z. Liu and R. Balasubramanian, *Proced. Environ. Sci.*, **16**, 159 (2012).
25. Z. Liu, A. Quek, S. Kent Hoekman and R. Balasubramanian, *Fuel*, **103**, 943 (2012).
26. K. Tekin, S. Karagöz and S. Bektaş, *Renew. Sustain. Energy Rev.*, **40**, 673 (2014).
27. C. Tian, B. Li, Z. Liu, Y. Zhang and H. Lu, *Renew. Sustain. Energy Rev.*, **38**, 933 (2014).
28. Z. Shuping, W. Yulong, Y. Mingde, I. Kaleem, L. Chun and J. Tong, *Energy*, **35**, 5406 (2010).
29. P. McKendry, *Bioresour. Technol.*, **83**, 37 (2002).
30. S. H. Chang, *Biomass. Bioenergy*, **62**, 174 (2014).
31. S. Kang, X. Li, J. Fan and J. Chang, *Ind. Eng. Chem. Res.*, **51**, 9023 (2012).
32. N. D. Berge, K. S. Ro, J. Mao, J. R. Flora, M. A. Chappell and S. Bae, *Environ. Sci. Technol.*, **45**, 5696 (2011).
33. M. Sevilla, J. A. Maciá-Agulló and A. B. Fuertes, *Biomass. Bioenergy*, **35**, 3152 (2011).
34. A. Demirbas, *Energy Convers. Manage.*, **49**, 2106 (2008).
35. Q. Xu, Q. Qian, A. Quek, N. Ai, G. Zeng and J. Wang, *ACS Sustain. Chem. Eng.*, **1**, 1092 (2013).
36. A. Fuertes, M. C. Arbestain, M. Sevilla, J. Maciá-Agulló, S. Fiol, R. López, R. J. Smernik, W. Aitkenhead, F. Arce and F. Macias, *Soil.*

Res., **48**, 618 (2010).
37. Z. Liu, A. Quek, S. Kent Hoekman and R. Balasubramanian, *Fuel*, **103**, 943 (2013).
38. G. K. Parshetti, S. Chowdhury and R. Balasubramanian, *Bioresour. Technol.*, **161**, 310 (2014).
39. G. K. Parshetti, S. Kent Hoekman and R. Balasubramanian, *Bioresour. Technol.*, **135**, 683 (2012).
40. C. Everard, C. Fagan, C. O'Donnell, D. O'Callaghan and J. Lyng, *J. Food Eng.*, **75**, 415 (2006).
41. Y. Wang, T. D. Wig, J. Tang and L. M. Hallberg, *J. Food Eng.*, **57**, 257 (2003).
42. M. Pala, I. C. Kantarli, H. B. Buyukisik and J. Yanik, *Bioresour. Technol.*, **161**, 255 (2014).
43. A. Arami-Niya, F. Abnisa, M. S. Shafeeyan, W. Daud and J. N. Sahu, *BioResources.*, **7**, 0246 (2012).
44. S. Marx, I. Chiyanzu and N. Piyo, *Bioresour. Technol.*, **164**, 177 (2014).
45. D. T. Chadwick, K. P. McDonnell, L. P. Brennan, C. C. Fagan and C. D. Everard, *Renew. Sustain. Energy Rev.*, **30**, 672 (2014).
46. J. Park, S. W. Won, J. Mao, I. S. Kwak and Y.-S. Yun, *J. Hazard. Mater.*, **181**, 794 (2010).
47. T. Zhang, W. P. Walawender, L. Fan, M. Fan, D. Daugaard and R. Brown, *Chem. Eng. J.*, **105**, 53 (2004).
48. W. M. A. W. Daud, W. S. W. Ali and M. Z. Sulaiman, *Carbon*, **38**, 1925 (2000).
49. K. Kirtania, J. Joshua, M. A. Kassim and S. Bhattacharya, *Fuel Process. Technol.*, **117**, 44 (2014).
50. A. C. Lua and T. Yang, *J. Colloid Interface Sci.*, **276**, 364 (2004).
51. K. Rashid, K. Reddy, A. Al Shoaibi and C. Srinivasakannan, *Can. J. Chem. Eng.*, **92**, 426 (2014).
52. W. Li, K. Yang, J. Peng, L. Zhang, S. Guo and H. Xia, *Ind. Crop. Prod.*, **28**, 190 (2008).
53. M. Sevilla, A. Fuertes and R. Mokaya, *Energy Environ. Sci.*, **4**, 1400 (2011).
54. S. S. Idris, N. A. Rahman, K. Ismail, A. B. Alias, Z. A. Rashid and M. J. Aris, *Bioresour. Technol.*, **101**, 4584 (2010).
55. M. n. Lapuerta, J. J. Hernandez and J. n. Rodríguez, *Biomass. Bioenergy*, **27**, 385 (2004).
56. L. Sanchez-Silva, D. López-González, J. Villasenor, P. Sanchez and J. Valverde, *Bioresour. Technol.*, **109**, 163 (2012).
57. H. Yang, R. Yan, H. Chen, D. H. Lee and C. Zheng, *Fuel*, **86**, 1781 (2007).
58. M. Mohammed, A. Salmiaton, W. Wan Azlina and M. Mohamad Amran, *Bioresour. Technol.*, **110**, 628 (2012).
59. S. A. El-Sayed and M. Mostafa, *Energy Convers. Manage.*, **85**, 165 (2014).
60. M. Asadieraghi and W. M. A. Wan Daud, *Energy Convers. Manage.*, **82**, 71 (2014).
61. Z. Liu, A. Quek and R. Balasubramanian, *Appl. Energy*, **113**, 1315 (2014).